(*From the* QUARTERLY JOURNAL OF THE ROYAL METEOROLOGICAL SOCIETY, Vol. 105, No. 443, January 1979)
Quart. J. R. Met. Soc. (1979), **105**, pp. 147–167
551.521:551.583:515.1

Catastrophes and resilience of a zero-dimensional climate system with ice-albedo and greenhouse feedback

By KLAUS FRAEDRICH
Institut für Meteorologie, Freie Universität Berlin
D-1000 Berlin 33

(Received 7 March 1978; revised 27 June 1978)

SUMMARY

An 'almost trivial' climate system of geometrical dimension zero is analysed. It consists of the global energy storage which is balanced by the globally averaged net radiation (solar input minus infrared emission) with ice-albedo and greenhouse feedbacks included. This nonlinear and time-dependent climate system is formulated as a gradient system of a potential. It can be analysed without explicit time integration according to catastrophe theory, so that the resilience of the system, due to changes of the external parameters and due to variations of the state variable, can be determined. For the ice-albedo or the greenhouse feedback alone, two equilibrium solutions appear: the stable ones are attractors, characterizing the present day interglacial; the unstable ones define a lower or an upper bound, respectively, for temperature changes to be absorbed by the systems. Beyond thresholds of external parameters (fold catastrophes) no equilibria exist, so that the systems attain the states of 'deep freeze' and 'desert heat', respectively. The two feedbacks combined lead to three equilibria, the stable interglacial being bounded by two unstable solutions, beyond which initial temperature values tend towards the 'deep freeze' or 'desert heat'. External parameter changes can lead to structural instability occurring at fold lines, which meet at the cusp catastrophe. Outside the fold and cusp catastrophes only unstable equilibria appear, from which initial temperature values tend towards 'desert heat' or 'deep freeze' situations.

1. INTRODUCTION

Chance and necessity cooperate to achieve climate variations – both stochastic and deterministic aspects have to be considered in the analysis of climate systems. Their effects on the structural behaviour of the system can be determined by resiliences (e.g. Grümm 1976) which are due to changes in the state variables (or uncertainties of the initial conditions) and due to changes of the external parameters (or boundary conditions). As an example of such an analysis a simple climate system of geometrical dimension zero is derived, describing the dynamics of a single state variable – the global mean temperature. An earlier paper (Fraedrich 1978) is extended by parameterizations of two temperature-dependent feedback mechanisms which are adopted from the literature, leading to a gradient system for the internal climate state variable. Here it should be realized that it is the main purpose of this paper to show qualitative aspects of the global climate system and its feedbacks; not to simulate quantitative details. An analysis of this zero-dimensional climate system has to include the effects of fluctuations of the internal variable and variations of external parameters: the origin of external parameter variations can be attributed to relatively slow changes due to astronomical or anthropogenic processes. The analysis of external parameter changes exhibits singularities (of smooth maps) which are called catastrophes. The analysis is completed by allowing for state variable fluctuations; the physical origin of a fluctuating global mean temperature may be ascribed to large-scale atmospheric or oceanic processes induced, e.g., by blocking action or anomalies of tropical circulation patterns. This part of the analysis leads to limits for state variable fluctuations beyond which the system attains a different structure. These limits depend on the external parameters only; here, they are defined by the unstable solutions.

In section 2 the basic climate system and the two feedback mechanisms are introduced. Later sections describe a sequence of models with these feedbacks; the structure and the resilience of the feedback systems are discussed with respect to changes of external parameters and the internal variable. In section 7 some practical aspects of sensitivity and stochastic forcing are discussed.

2. Zero-dimensional climate system

A global climate system of geometrical dimension zero can be described by the energy conservation law after integrating over the total mass (per unit area) of the system:

$$c\,dT/dt = R\downarrow - R\uparrow \qquad (2.1)$$

(For definitions of symbols see appendix.) The storage term (left) results from the imbalance between net incoming solar radiation, $R\downarrow$, and outgoing emission, $R\uparrow$.

The storage term characterizes the time-dependent behaviour of the system, its dynamics being described by the single internal (or state) variable, T. The state variable is interpreted as an average surface temperature of, e.g., an ocean on a spherical planet which is subject to radiative heating. This allows storage to be simplified by a constant thermal inertia, $c > 0$, if a mixed reservoir of fixed depth h and area coverage α is considered:

$$c = \rho_m c_m h \alpha \qquad (2.2)$$

Incoming solar radiation,

$$R\downarrow = \tfrac{1}{4}\mu I_0(1-\alpha_p), \qquad (2.3)$$

is modified by an external parameter, μ, to allow for variations in the solar constant, I_0, or for long-term variations of the planetary orbit (von Woerkom 1953). Unless the planetary albedo, α_p, is taken as an external parameter, an ice-albedo feedback has to be introduced to link variations in temperature with changes of ice (and/or cloudiness) and thus of albedo:

$$\alpha_p = a_2 - b_2 T^2 \qquad (2.4)$$

The linear feedback $\alpha_p = a_1 - b_1 T$ introduced to climate modelling by Budyko (1969) and Sellers (1969) is replaced by a quadratic relation of the same slope, $b_1 = 2b_2T_0$, and same value, α_p, at present day, T_0, conditions. Some reasons for introducing Eq. (2.4) may be mentioned: (i) The quadratic feedback is similar to the greenhouse effect (discussed later in this section), modifying the effective emissivity. (ii) This formulation leads to simple and analytic expressions for the equilibria of the feedback models to be discussed in the following sections. (iii) There is hardly any qualitative difference in the structure for the equilibria using either parameterization. (iv) Within a realistic temperature interval, there are only small differences between the quadratic and linear ice-albedo feedbacks. This is shown in Fig. 1 for present day conditions, external parameters being indicated by the additional subscript '$_0$'.

Infrared emission is better correlated with the mass-averaged temperature of the atmosphere than with the surface temperature. But it is the surface temperature which determines the formation of ice and which is therefore used in the following parameterizations. This leads to a net outgoing longwave radiation $R\uparrow$ determined by a contribution from the surface, $L\uparrow = \varepsilon_s\sigma T^4$, and diminished by atmospheric counter-radiation, $L\downarrow = \varepsilon_a\sigma T^4$:

$$R\uparrow = \varepsilon_{sa}\sigma T^4 \qquad (2.5)$$

where the effective emissivity $\varepsilon_{sa} = \varepsilon_s - \varepsilon_a$. The longwave emission from the surface, $L\uparrow$, is prescribed by a Stefan–Boltzmann law with surface emissivity ε_s; atmospheric radiation, $L\downarrow$, is assumed to be proportional to blackbody surface emission (ε_a: atmospheric emittance). Unless the atmospheric emittance in Eq. (2.5) is assumed to be an external parameter,

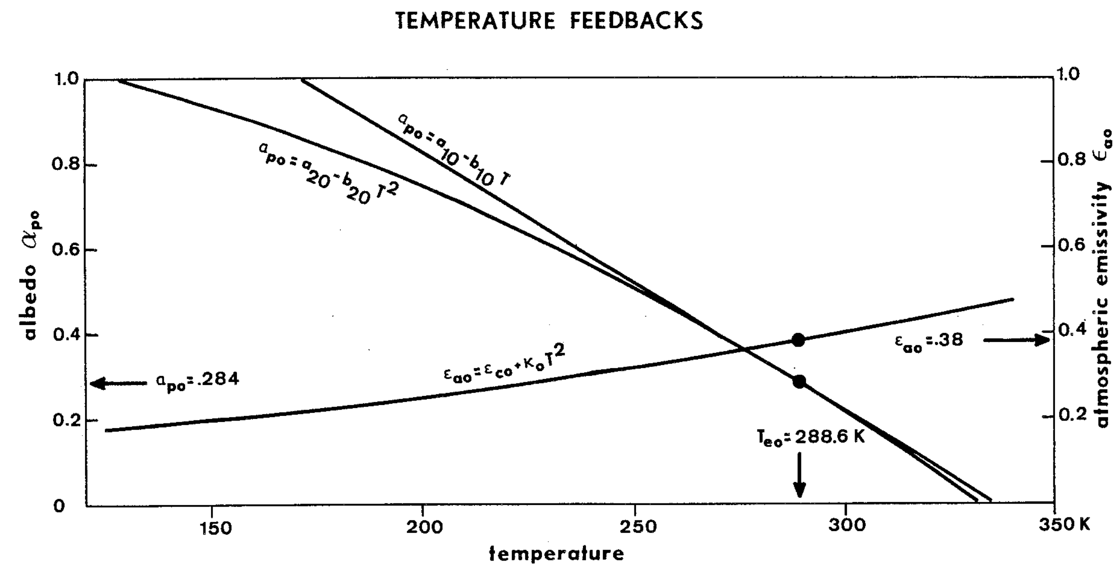

Figure 1. External parameters at 'present day' reference conditions (subscript '$_0$'): temperature-dependent planetary albedo (ice-albedo feedback) and atmospheric emittance (greenhouse effect).

atmospheric radiation, $L\downarrow$, has to be parameterized; we use Swinbank's (1963) empirical formula $L\downarrow \sim T^6$, the theoretical derivation of which has been attempted by Deacon (1970). This allows us to represent the greenhouse effect of longwave counter-radiation by a temperature-dependent feedback for the atmospheric emittance ε_a, $\sim T^2$. Such a temperature feedback allows for variations in the amount of water vapour, which is closely related to temperature. The effect of carbon dioxide may be considered separately, using the following formulation for CO_2 emittance, $\varepsilon_c = 0{\cdot}0235 \ln(CO_2)$, CO_2 in ppm, where a correction for band-overlap has been incorporated (for details see Bryson and Dittberner 1976). This combination leads to a temperature feedback parameterization for the greenhouse effect:

$$\varepsilon_a = \varepsilon_c + \kappa T^2 \quad . \quad . \quad . \quad . \quad . \qquad (2.6)$$

It is obvious that this feedback mechanism shows, apart from its sign, similaiity to the ice-albedo feedback, Eq. (2.4). As the parameterization (2.6) is based upon Swinbank's formula, it is subject to the assumption of a clear sky. In the following it will be presumed that this parameterization can be generalized to global conditions such that its structure ($\sim T^6$) is not altered, i.e. only empirical (external) parameters are allowed to vary. An adjustment to present day conditions is presented in section 3. Again, it should be emphasized that it is the main purpose of this paper to show the qualitative effect of the greenhouse feedback on the structural behaviour of the zero-dimensional climate system.

A general comment seems appropriate on the ice-albedo and greenhouse feedback mechanisms (Eqs. (2.4) and (2.6)) characterizing the climatic sub-systems cryosphere, hydrosphere and atmosphere. It is implicitly assumed that both the extent of the cryosphere (ice-albedo feedback) and the amount of water vapour in the atmosphere (greenhouse effect) instantaneously respond to changes in T. Additionally, the storage term is given by a constant thermal inertia of the hydrosphere. Thus, the description of the dynamics of this model is confined to the three climatic sub-systems being in equilibrium with each other.

The zero-dimensional climate system is obtained by combining Eqs. (2.1), (2.3) and (2.5). Introducing the parameterizations of the ice-albedo feedback, Eq. (2.4), and the greenhouse effect, Eq. (2.6), a series of climate systems can be investigated. They all take the general form of a gradient system which evolves according to

$$dT/dt = f(T;x) \qquad (2.7)$$

for fixed external parameters $x = (\mu, \alpha_p, a_2, b_2, \varepsilon_s, \varepsilon_a, \varepsilon_c, \kappa, c)$, not all of which will appear in any one problem.

The method of analysis of Eq. (2.7) follows the principles of catastrophe theory, according to which the geometrical structure of a gradient system $f(T) = -dV/dT$ of a potential $V(T)$ can be described and classified (see, e.g., Thom 1975):

(i) The set of equilibria (fixed points) $T_e(x)$ satisfying

$$f(T_e;x) = 0 \qquad (2.8)$$

is a k-dimensional surface (k: number of external parameters) in the $(1+k)$-dimensional state space with one internal variable. These equilibria appear as the extrema of the potential $V(T_e)$ where $dV/dT|_{T_e} = 0$.

(ii) A criterion for the internal stability of equilibria can be deduced from the linearized version of the basic climate equation (2.8), obtained by a truncated Taylor series expanded about the equilibrium $f(T_e;x) = 0$:

$$dT/dt = f(T_e)+(df/dT)|_{T_e}(T-T_e)+ \ldots \doteqdot -\lambda(T-T_e).$$

The eigenvalue

$$-\lambda = (df/dT)|_{T_e} \begin{matrix} > 0 \text{ unstable} \\ < 0 \text{ stable} \end{matrix} \qquad (2.9)$$

characterizes the time-dependent behaviour of the linearized climate system at the equilibrium T_e for fixed external parameters. The inverse of the eigenvalue $\tau_c = \lambda^{-1}$ defines the (e-folding) time scale according to which the state variable T approaches (leaves) the stable (unstable) equilibrium, in the neighbourhood of which the nonlinear system behaves locally like a linear one. The criterion (2.9) is equivalent to a sufficient condition for the extremum of the potential V to be a minimum: $d^2V/dT^2 = -\lambda < 0$ (attractor), or a maximum: $d^2V/dT^2 = -\lambda > 0$ (repeller).

(iii) The dynamics of time-dependent behaviour of the gradient system $f(T)$ can be displayed by a phase portrait. In the following analysis it shows a temperature tendency $c\,dT/dt$ in terms of the temperature-dependent difference between incoming and outgoing radiation, $R\downarrow - R\uparrow \gtrless 0$. This leads to the concept of resilience in state space, or prediction of the first kind (e.g. Lorenz 1975; Grümm 1976; Holling 1973). With fixed external parameters, all initial values which depart from the equilibria (i.e. $R\downarrow - R\uparrow \neq 0$) lead to a temperature flow $T(t)$ away from a repeller and towards an attractor. The sign of the difference $R\downarrow - R\uparrow$ gives the direction of the flow with increasing ($dT/dt > 0$) or decreasing ($dT/dt < 0$) temperature. The magnitude of this difference gives a measure of the repelling or attracting forces, i.e. the angles at which $R\downarrow$ and $R\uparrow$ cross the equilibria ($R\downarrow = R\uparrow$) represent the characteristic time scale $\lambda^{-1} = \tau_c$, Eq. (2.9). As will be shown in later sections, the system without any feedback at all has the strongest attracting power, indicated by a short time scale but large $R\downarrow - R\uparrow$ for T approaching T_e. The weakest attracting and repelling power is attributed to the system where the feedbacks oppose each other.

(iv) Singularities of the equilibria are defined in the state space $(T_e;x)$ by $-\lambda = (df/dT)|_{T_e} = 0$. This is equivalent to a condition for which the maximum and minimum of the potential $V(T_e)$ coincide: $d^2V/dT^2 = 0$. These singularities can be projected on to the external parameter space (x) by eliminating T_e from

$$(df/dT)|_{T_e} = 0 \text{ and } f(T_e) = 0 \qquad (2.10)$$

The combination (2.10) provides the condition for structural instability which, in the parameter space, describes the location of sudden catastrophic jumps of the (set of) equilibria. These catastrophes occur whenever external parameters are forced to cross these (projections of the) singularities, Eq. (2.10), which define, e.g., a line or surface in the parameter plane or space. Thus, the system can absorb changes in the parameters (i.e. it keeps structurally stable) unless parameter trajectories cross the hyperplane (2.10), where the equilibria are structurally unstable. This introduces the concept of resilience of state space or the prediction of the second kind.

In what follows, two types of singularity of equilibria (elementary catastrophes) appear: fold catastrophe and cusp catastrophe. The fold catastrophe emerges at a bifurcation point where two branches of stable and unstable equilibria coalesce. It is determined by the condition (2.10). The cusp catastrophe emerges at the bifurcation point where two branches of fold catastrophe (fold-lines) coalesce; it is given by the condition:

$$f(T_e) = 0; \quad (df/dT)|_{T_e} = 0; \quad (d^2f/dT^2)|_{T_e} = 0 \qquad (2.11)$$

Projection into the parameter space (i.e. the related parameter combination for the cusp) is obtained by eliminating the equilibrium state variable T_e from Eqs. (2.11). The above subsections are illustrated in the sketch shown in Fig. 6 (after Bröcker 1975).

3. Trivial climate system and feedback calibration

The trivial zero-dimensional climate system without feedback is obtained from Eqs. (2.1), (2.3) and (2.5):

$$dT/dt = (1/c)\{-\varepsilon_{sa}\sigma T^4 + \tfrac{1}{4}\mu I_0(1-\alpha_p)\} \qquad (3.1)$$

The equilibrium solution $f(T_e) = 0$ of Eq. (3.1) leads to the simple fourth-order polynomial

$$T_e^4 - (\tfrac{1}{4}\mu I_0/\varepsilon_{sa}\sigma)(1-\alpha_p) = 0 \qquad (3.2)$$

which depends on three external parameters $x = (\alpha_p, \varepsilon_{sa}, \mu)$ reduced to one combination. There exists only one physically realistic root of Eq. (3.2),

$$T_e = +\{(\tfrac{1}{4}\mu I_0/\varepsilon_{sa}\sigma)(1-\alpha_p)\}^{\frac{1}{4}}, \qquad (3.3)$$

which is internally stable because

$$-\lambda = (df/dT)|_{T_e} = -(\varepsilon_{sa}\sigma/c)\,4T_e^3 < 0 \qquad (3.4)$$

Thus for all initial values $T > 0$, and at fixed external parameters, the temperature approaches the stable equilibrium (attractor) T_e, Eq. (3.3). The singularity at $T_e = 0$ is unrealistic, and trivial, because a fold catastrophe occurs at $(\tfrac{1}{4}\mu I_0/\varepsilon_{sa}\sigma)(1-\alpha_p) = 0$, i.e. there are no real solutions for a negative argument in Eq. (3.3). There will be no further consideration of this singularity.

A reference situation (subscript '$_0$') is defined by the external parameter combination $x_0 = \{\alpha_{p0} = 0{\cdot}284, \varepsilon_{sa0} = 0{\cdot}62, \mu_0 = 1\}$. Using the trivial climate system (3.3) these values lead to the globally averaged 'present day' equilibrium temperature $T_{e0} = 288{\cdot}6$ K. The planetary albedo $\alpha_{p0} = 0{\cdot}284$ is taken from Raschke *et al.* (1973); this gives an effective emissivity $\varepsilon_{sa0} = 0{\cdot}62$. A thermal inertia for the zero-dimensional climate systems (2.2) is derived for a well-mixed ocean layer of depth $h = 30$ m covering $\alpha = 70{\cdot}8\%$ of the earth's surface: $c_0 = 10^8 \mathrm{kg\,K^{-1}s^{-2}}$.

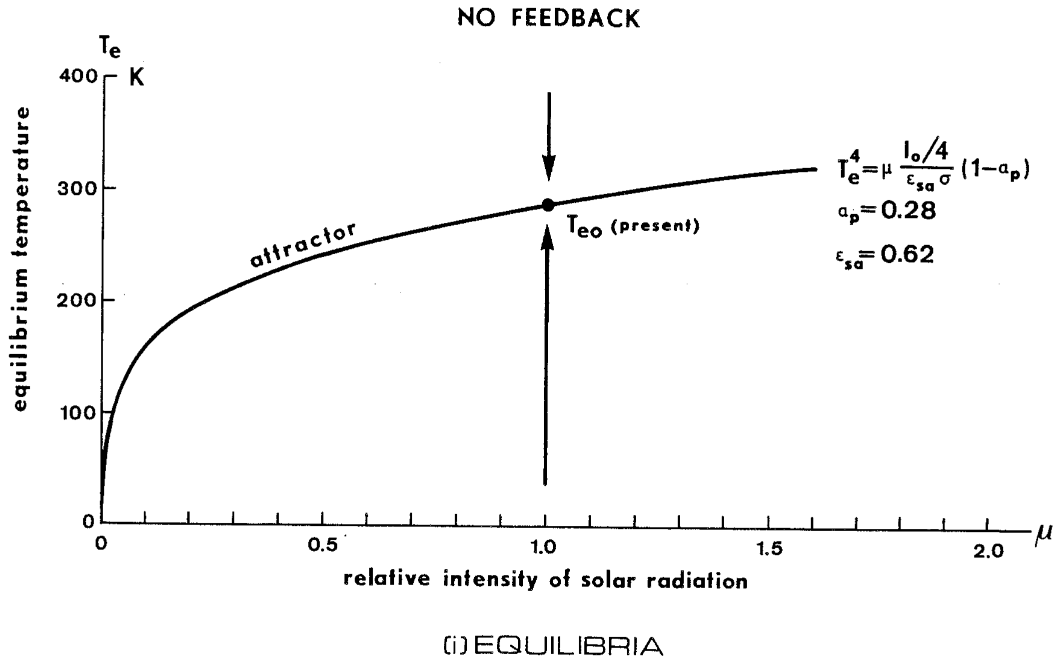

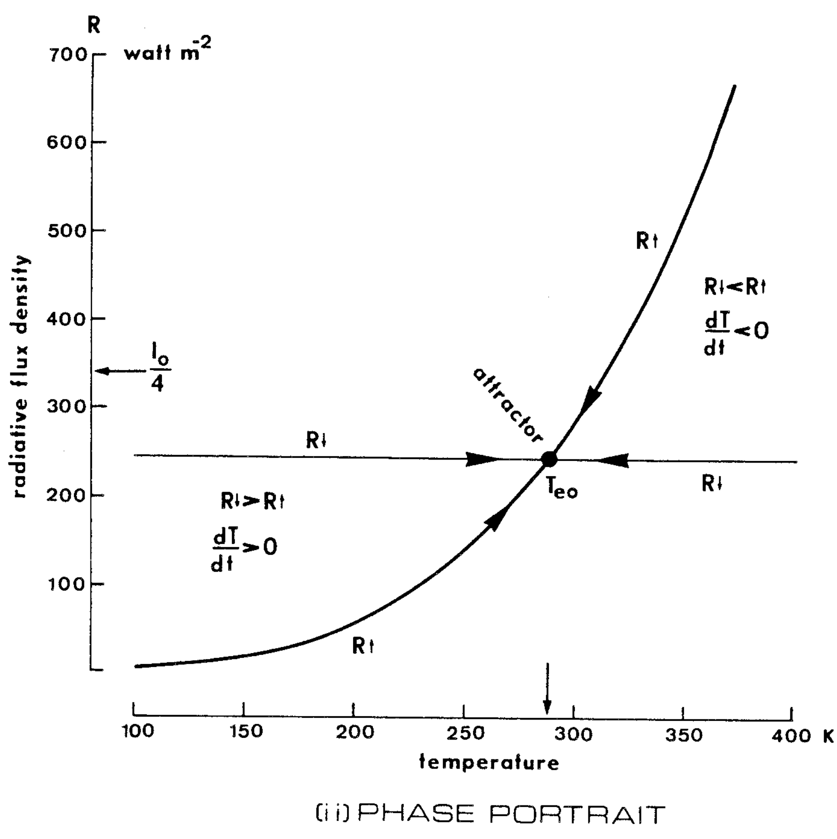

Figure 2. Climate system with no feedback: (i) equilibria (cross-section through state space); (ii) ph portrait at reference conditions. (For detailed description see Fig. 3 and text.)

For present day albedo and emissivity the equilibrium solution (3.3) of the trivial climate system is presented (Fig. 2), varying with the relative intensity, μ, of solar radiation. The phase portrait (Fig. 2) displays the attractor (stable equilibrium) for the reference condition in terms of the incoming, $R\downarrow$, and temperature-dependent outgoing radiation, $R\uparrow$, so that the temperature flow (i.e. the tendency $dT/dt \gtrless 0$) is determined by the radiation imbalance $R\downarrow - R\uparrow$. The characteristic time scale according to which the linearized version of the trivial climate system approaches the reference situation T_{e0} is $\tau_{c0} = \lambda_0^{-1} = 1{\cdot}4$ yr. From Eqs. (3.3) and (3.4) it is obvious that the system (3.1) can absorb changes of the state variable where all initial conditions $T > 0$ have trajectories to the attracting stable equilibrium T_e (resilience of the first kind); additionally, the system can absorb changes of the external parameters as long as $\frac{1}{4}\mu I_0(1-\alpha_p)/\varepsilon_{sa}\sigma > 0$ without structural instability occurring (resilience of the second kind). This behaviour can be simply interpreted by the potential, V, of Eq. (3.2), the only minimum of which is the equilibrium (3.3), attracting all temperature flows.

The reference situation allows a calibration of the two temperature feedback mechanisms which are discussed in the following sections. To deduce the reference magnitudes of the ice-albedo feedback parameters a_{20} and b_{20}, Eq. (2.4), two requirements have to be satisfied: at present day conditions the slope and the value of the quadratic and linear ice-albedo feedback have to correspond:

$$\alpha_{p0} = a_{20} - b_{20}T_{e0}^2 \qquad (3.5a)$$

$$(d\alpha_p/dT)\big|_{T_{e0}} = -b_{10} = -2b_{20}T_{e0} \qquad (3.5b)$$

With $\alpha_{p0} = 0{\cdot}284$, $b_{10} = 0{\cdot}006\,\mathrm{K}^{-1}$ at $T_{e0} = 288{\cdot}6\,\mathrm{K}$ (see, e.g., Lian and Cess 1977) one obtains $a_{20} = 1{\cdot}2$, $b_{20} = 0{\cdot}1 \times 10^{-4}\mathrm{K}^{-2}$.

The reference magnitudes of the parameters ε_{c0} and κ_0 for the greenhouse effect can also be derived, if two requirements are fulfilled satisfying the 'present day', T_{e0}, situation: the total atmospheric emittance, ε_{a0}, and the contribution, ε_{c0}, of CO_2, Eq. (2.6), to it:

$$\varepsilon_{a0} = \varepsilon_{c0} + \kappa_0 T_{e0}^2 \qquad (3.6a)$$

$$\varepsilon_{c0} = 0{\cdot}13 \qquad (3.6b)$$

where the present CO_2 content (315 ppm) has been introduced to yield ε_{c0}. With $\varepsilon_{a0} = 0{\cdot}38$ one obtains $\kappa_0 = 3{\cdot}0 \times 10^{-6}\mathrm{K}^{-2}$. A simple rearrangement, dealing with the external parameters for the emissivities, appears useful: $\varepsilon_{sa0} = (\varepsilon_s - \varepsilon_a)_0 = (\varepsilon_s - \varepsilon_c)_0 - \kappa_0 T_{e0}^2 = \varepsilon_{sc0} - \kappa_0 T_{e0}^2$, so that $\varepsilon_{sc0} = 0{\cdot}87$.

4. Ice-albedo feedback

The climate system with linear ice-albedo feedback has already been extensively analysed (Fraedrich 1978). Therefore, the quadratic feedback (2.4) is introduced into the basic climate system (3.1) and will briefly be discussed in this section:

$$dT/dt = (1/c)\{-\varepsilon_{sa}\sigma T^4 + \tfrac{1}{4}\mu I_0 b_2 T^2 + \tfrac{1}{4}\mu I_0(1-a_2)\} \qquad (4.1)$$

The equilibria $f(T_e) = 0$ of Eq. (4.1) can be deduced from the biquadratic polynomial

$$T_e^4 - mT_e^2 + n = 0 \qquad (4.2a)$$

where $m = (\frac{1}{4}\mu I_0/\varepsilon_{sa}\sigma)b_2$; $n = -(\frac{1}{4}\mu I_0/\varepsilon_{sa}\sigma)(1-a_2)$ (4.2b)

The equilibria depend on the four external parameters $x = (a_2, b_2, \varepsilon_{sa}, \mu)$, which can be

(a)

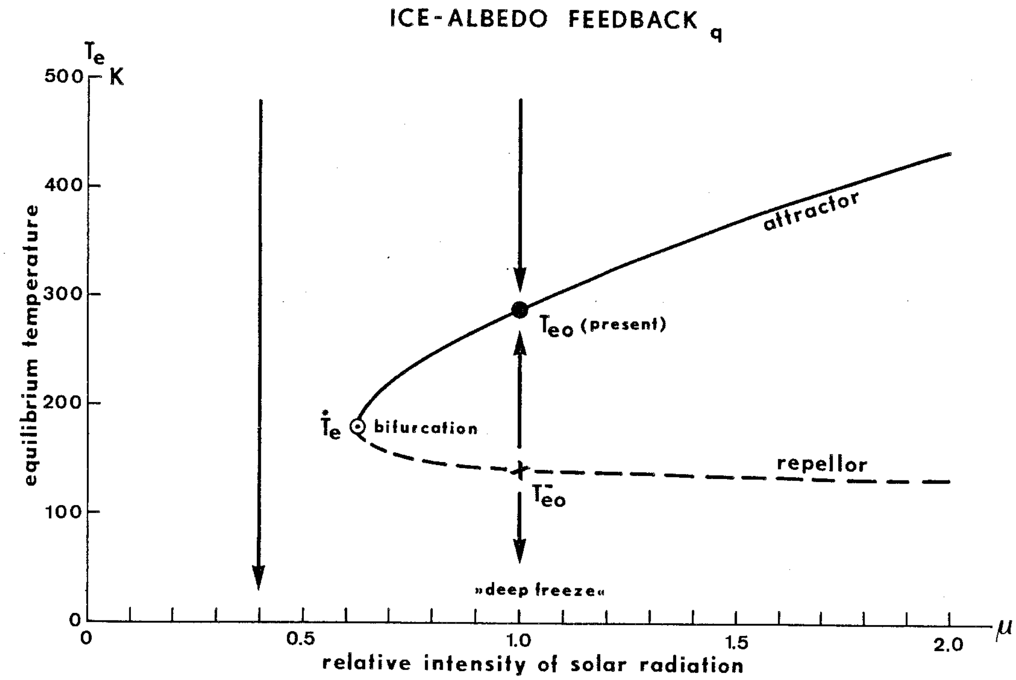

(i) EQUILIBRIA

(b)

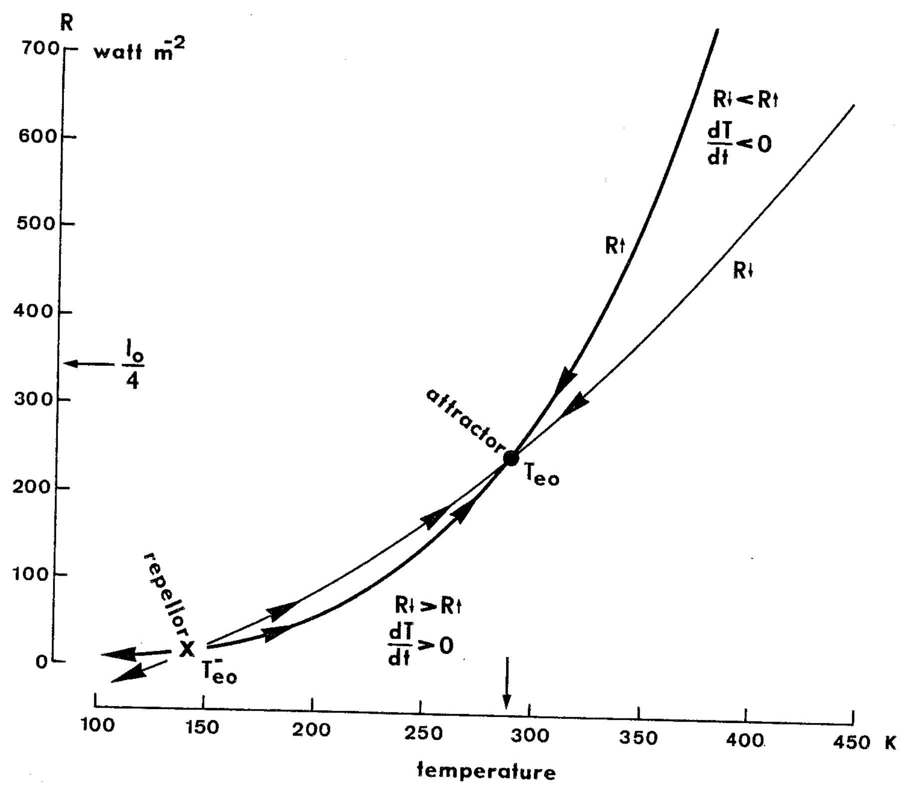

(ii) PHASE PORTRAIT

(c)

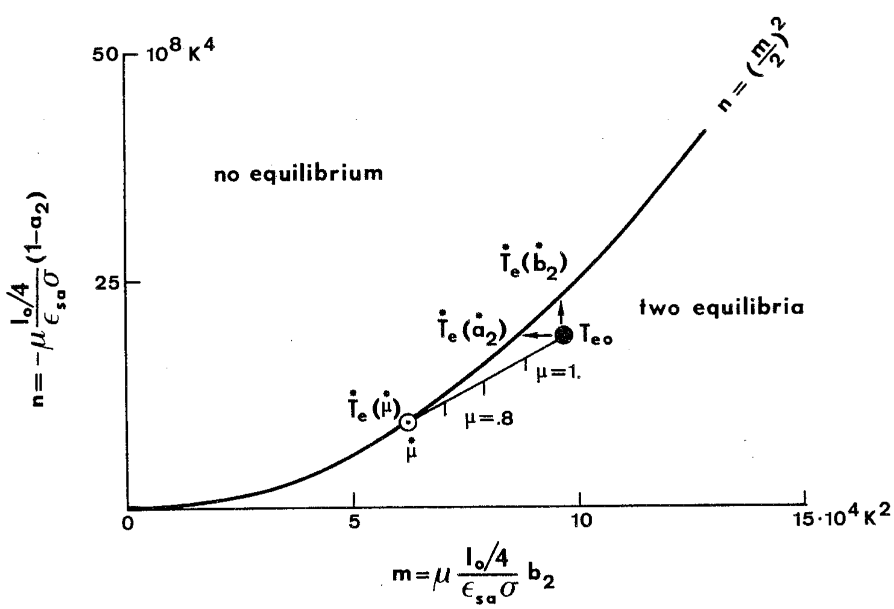

(iii) BIFURCATION DIAGRAM

Figure 3. Climate system with ice-albedo feedback: (a) The equilibria represent a cross-section through the state space, depending only on the intensity of solar radiation. (b) A phase portrait shows the temperature tendency in terms of the incoming, $R\downarrow$, and outgoing, $R\uparrow$, radiation at present day conditions. (c) The bifurcation diagram shows the singularities of the equilibria projected onto the parameter plane.

reduced to the two combinations (m, n) not involving c. The physically realistic roots of Eqs. (4.2) are

$$T_e^{\pm} = \{\tfrac{1}{2}m \pm (\tfrac{1}{4}m^2 - n)^{\frac{1}{2}}\}^{\frac{1}{2}}, \qquad (4.3)$$

which describe a surface in $(T_e; m, n)$ space. The two branches T_e^+ and T_e^- coalesce at the bifurcation line $\overset{*}{T}_e = T_e^+ = T_e^-$, where $m^2/4 = n$ (Fig. 3(a)). These equilibria, (4.3), are shown for changing solar radiation, μ, with all other external parameters kept at their reference values derived in section 3.

The internal stability (instability) of the equilibria (4.3) is defined by the negative (positive) eigenvalue

$$-\lambda = (df/dT)\big|_{T_e} = -(\varepsilon_{sa}\sigma/c)(T_e^2 - \tfrac{1}{2}m)4T_e \begin{matrix} < 0 \text{ stable} \\ > 0 \text{ unstable} \end{matrix} \qquad (4.4)$$

Thus, the upper (lower) branch T_e^+ (T_e^-) represents the set of stable (unstable) equilibrium solutions. For fixed external parameters (e.g. the reference condition) the phase portrait (Fig. 3(b)) shows the temperature tendency dT/dt in terms of the radiation balance $R\downarrow - R\uparrow$ for given initial temperature values. Thus, the unstable equilibrium T_{eo}^- defines the repeller as a lower bound for initial values from which the temperature flow tends towards the stable solution T_{eo}^+ (attractor); there is no such upper bound, because all initial values $T > T_{eo}^+$ have trajectories towards T_{eo}^+. For initial values $T < T_e^-$ the temperature flow tends towards minus infinity ('deep freeze') unless the albedo–temperature feedback is cut off and, e.g., replaced by a constant albedo. The geometrical interpretation by a potential is obvious, because its minimum (maximum) is equivalent to the stable (unstable) equilibrium of the gradient system (4.1). The stable equilibrium may be identified with interglacial conditions, separated from the 'deep-freeze' by the unstable equilibrium. At 'present day' conditions, the characteristic time scale of the ice-albedo feedback system yields $\tau_{c0} = \lambda_0^{-1} = 2{\cdot}4\,\text{yr}$.

The singularities (i.e. sudden changes) of the equilibria (due to parameter variations only) reveal a bifurcation line in the state space $(T_e; m, n)$ where the stable and unstable equilibria sets coalesce. The related projection on to the parameter plane (m, n) can be simply derived by combining Eqs. (4.2) and (4.4) for $\lambda = 0$, eliminating T_e (see section 2). This leads to the condition of structural instability which depends on external parameters only, i.e. a fold catastrophe:

$$\tfrac{1}{4}m^2 - n = 0, \text{ or } (\tfrac{1}{4}\mu I_0/\varepsilon_{sa}\sigma)(\tfrac{1}{4}b_2^2)\{-(1-a_2)^{-1}\} = 1 \qquad (4.5)$$

The related bifurcation temperatures $\overset{*}{T}_e$ can be determined from Eqs. (4.4) with $\lambda = 0$. For $(m/2)^2 > n$, two equilibria exist, the internal stability of which has been discussed, Eqs. (4.4). At the bifurcation line, or fold catastrophe, $(m/2)^2 = n$, the local maximum and minimum of the potential V of the gradient system $f(T_e)$ coincide. For $(m/2)^2 < n$, however, these local extrema vanish, i.e. due to the imaginary root in Eq. (4.3) there are no equilibria. Thus, all initial values have a temperature flow leading to the 'deep freeze' situation. The direction of flow is due to the negative sign of the term with the highest power in T, Eq. (4.1); (see Fig. 3(a)).

With a continuously decreasing ice-albedo feedback ($b_2 \to 0$, $m \to 0$) the system (4.1) attains a structure similar to that of the trivial climate system. This can be visualized (see Fig. 3), because the bifurcation temperature $\overset{*}{T}_e = \sqrt{(m/2)}$ vanishes simultaneously with decreasing solar radiation (Eqs. (4.4), $\lambda = 0$; Eq. (4.5), $n \to 0$).

An example illustrates the structural behaviour of the climate system. If the relative intensity of solar radiation, μ, is assumed to change, and all other parameters are kept fixed at 'present day' conditions, the equilibria appear as a cross-section through $(T_e; m, n)$ space (Fig. 3(a)). The related variations of solar radiation intensity, projected on to the parameter space, are shown in Fig. 3(c), where they meet the fold line, Eq. (4.5), in the parameter plane at

$$\overset{*}{\mu} = \{4(1-a_2)/(-b_2)\}(1/b_2)(\varepsilon_{sa}\sigma/\tfrac{1}{4}I_0) \qquad (4.6)$$

The related equilibrium temperature at this bifurcation point is

$$\overset{*}{T}_e = \{4(1-a_2)/(-b_2)\}^{\frac{1}{2}}; \qquad (4.7)$$

i.e. for 'present day' conditions (section 3) the μ bifurcation lies at $\overset{*}{T}_e = 180\,\text{K}$ where $\overset{*}{\mu} = 0{\cdot}63$. Beyond the bifurcation $\mu < \overset{*}{\mu}$ there is no real equilibrium so that for any initial value the temperature of the system drops to a 'deep freeze' situation, unless the ice-albedo feedback is cut off at some realistic temperature or albedo threshold. Bifurcation points for other external parameters can also be deduced from Eqs. (4.2) and (4.5). Some of them are indicated in Fig. 3(c), where the remaining external parameters are in each case fixed at 'present day' conditions.

5. Greenhouse effect

If the greenhouse effect of the longwave atmospheric counter-radiation parameterized by Eq. (2.6) is incorporated into the basic climate system (3.1), and there is no ice-albedo feedback, one obtains

$$(dT/dt) = (1/c)\{\kappa\sigma T^6 - \varepsilon_{sc}\sigma T^4 + \tfrac{1}{4}\mu I_0(1-\alpha_p)\}, \qquad (5.1)$$

where $\varepsilon_{sc} = \varepsilon_s - \varepsilon_c$. The equilibria $f(T_e) = 0$ of Eq. (5.1) satisfy the sixth-order polynomial

$$T_e^6 - (\varepsilon_{sc}/\kappa)T_e^4 + (\tfrac{1}{4}\mu I_0/\kappa\sigma)(1-\alpha_p) = 0, \qquad (5.2a)$$

which can be transformed to the following normalized form of a cubic equation:

$$y^3 - uy + v = 0; \qquad y = -\varepsilon_{sc}/3\kappa + T_e^{2}, \qquad (5.2b)$$

where $u = 3(\varepsilon_{sc}/3\kappa)^2 > 0; \quad v = -2(\varepsilon_{sc}/3\kappa)^3 + (\frac{1}{4}\mu I_0/\kappa\sigma)(1-\alpha_p)$. (5.2c)

The equilibria depend on the five external parameters $x = (\alpha_p, \varepsilon_s, \varepsilon_c, \kappa, \mu)$, which reduce to two combinations (u, v). The roots of Eq. (5.2) lead to the following (positive!) equilibrium temperatures which represent a surface in the $(T_e; u, v)$ state space:

$$T_e = +\{\varepsilon_{sc}/3\kappa + 2(|u|/3)^{\frac{1}{2}}A\}^{\frac{1}{2}} \quad . \quad . \quad . \quad (5.3)$$

For $u > 0$ and $(v/2)^2 < (u/3)^3$ there exist three solutions of Eq. (5.3) with $A = \cos(\rho/3)$; $-\cos\{(\pi+\rho)/3\}$; $-\cos\{(\pi-\rho)/3\}$, where $\rho = \text{arc}\cos\{-(v/2)(u/3)^{-\frac{3}{2}}\}$, the last of which is imaginary. For $u > 0$ but $(v/2)^2 > (u/3)^3$ one solution appears with $A = \cosh(\rho/3)$, where $\rho = \text{Arcosh}\{-(v/2)(u/3)^{-\frac{3}{2}}\}$; but for $R\downarrow > 0$ it produces imaginary values. The remaining two real solutions represent a surface in the $(T_e; u, v)$ space. They are shown in Fig. 4 (equilibria) for changing solar radiation intensity, where all other external parameters are fixed and defined by the reference situation (section 3). The internal stability of the equilibria (5.3) is given by

$$-\lambda = (df/dT)|_{T_e} = (\kappa\sigma/c)\{T_e^2 - \tfrac{2}{3}(\varepsilon_{sc}/\kappa)\}\,6T_e^3 \begin{array}{l} < 0 \text{ stable} \\ > 0 \text{ unstable} \end{array} \quad . \quad (5.4)$$

so that the upper branch, T_e^+ (Fig. 4(a)), represents unstable solutions (repeller). For all external parameters fixed at the reference condition, the phase portrait (Fig. 4(b)) shows the temperature tendency dT/dt. It is correlated with the radiation balance $R\downarrow - R\uparrow$, Eq. (2.1), and thus depends on the (initial) temperature values. The unstable equilibrium, T_e^+, appears as a repeller corresponding to an upper bound for initial values from which the temperature flow tends towards the stable solution T_{e0}^- (attractor). For initial values beyond the repeller, $T > T_e^+$, the temperature flow tends towards plus infinity ('desert heat')* unless the greenhouse effect is cut off and, e.g., replaced by a constant atmospheric emittance ε_a. For 'present day' conditions the characteristic time scale of the greenhouse feedback system yields $\tau_{c0} = \lambda_0^{-1} = 1{\cdot}8$ yr.

The resilience of the state space (prediction of the second kind) determines the reaction of the system to changes of the external parameters. It can be discussed in terms of the singularities ($\lambda = 0$) of the equilibria in the $(T_e; u, v)$ state space. If projected on to the parameter plane (u, v), these singularities appear as fold catastrophes which can be determined from Eqs. (5.2b) and (5.4), $\lambda = 0$:

$$(\tfrac{1}{3}u)^3 = (\tfrac{1}{2}v)^2, \text{ or } (\tfrac{1}{4}\mu I_0/\varepsilon_{sc}\sigma)(1-\alpha_p) = \tfrac{1}{3}(2\varepsilon_{sc}/3\kappa)^2 \quad . \quad (5.5)$$

The related bifurcation temperature is given by Eqs. (5.4), $\lambda = 0$, i.e. $\overset{*}{T}_e = (2\varepsilon_{sc}/3\kappa)^{\frac{1}{2}}$. For parameters satisfying $(v/2)^2 < (u/3)^3$, two real equilibria can be determined, one of which is the attractor. The third solution is imaginary ($T_e^2 < 0$) and will be excluded from the discussion.

An appropriate picture in the parameter plane is presented in Fig. 4(c): $(v/2)^2 < (u/3)^3$ appears as the area spanned between the fold lines; outside the fold lines, for $(v/2)^2 > (u/3)^3$, only one (or no) equilibrium temperature appears, provided there is one (or no) real temperature value.

The external parameter regions $(v/2)^2 \gtrless (u/3)^3$ are separated by the structural instability condition (Eq. (5.5), Fig. 4(c)), across which small external parameter variations lead to a structure change of the equilibria in the state space. For any parameter combination beyond the bifurcation lines, initial temperature values $T > 0$ tend towards infinity, whereas for $(v/2)^2 < (u/3)^3$ there is always one attractor, but also one (real) repeller. Whether the temperature increases or decreases depends on the situation of the initial value with respect to the repeller (unstable equilibrium). Here, it is the 'desert heat' state (plus infinity) which will always be approached until the feedback is cut off.

* 'boiling heat' may be as illustrative.

Physically, the stable equilibrium (attractor T_e^-) can be identified with interglacial climate. It is separated from the 'desert heat' by the repeller T_e^+ if only variations of the internal variable at fixed external parameters are considered (prediction of the first kind, resilience in state space). If resilience of state space is discussed, i.e. if variations of external parameters are considered, the stable interglacial climate conditions or the attractor is

(a)

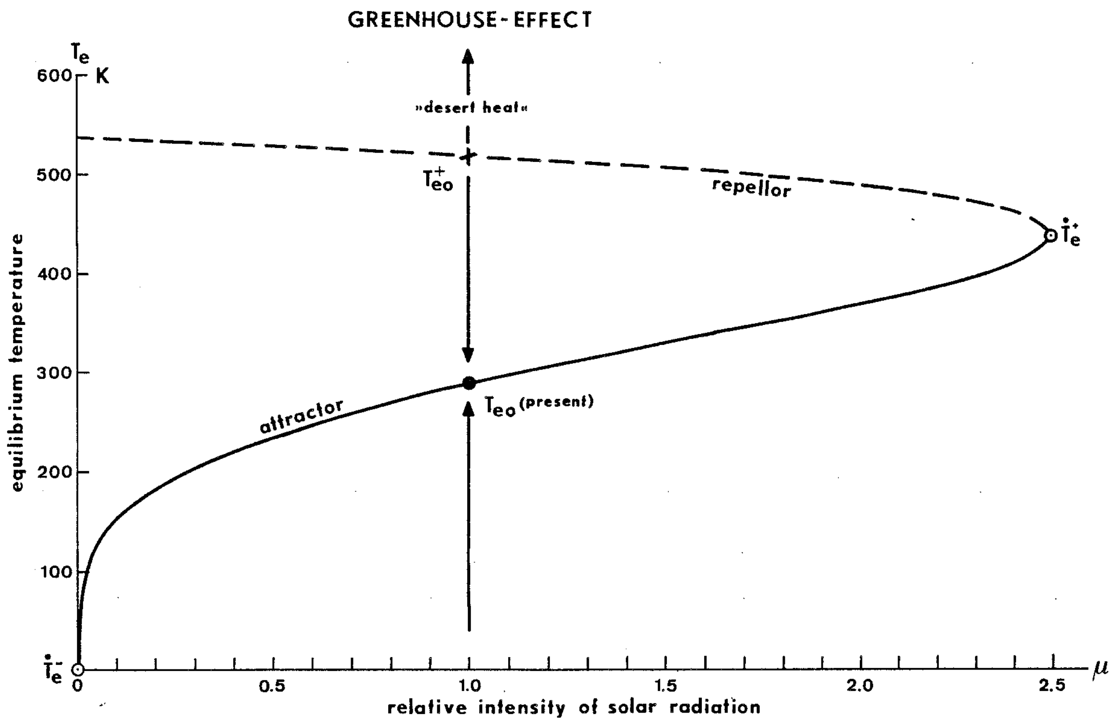

(i) EQUILIBRIA

(b)

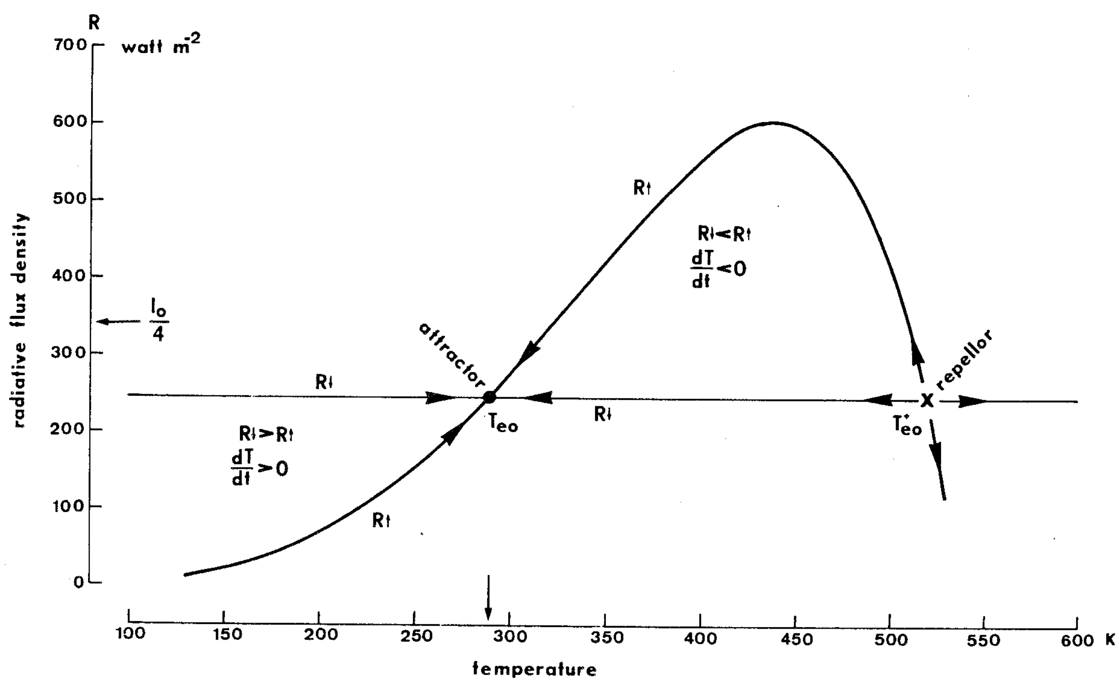

(ii) PHASE PORTRAIT

(c)

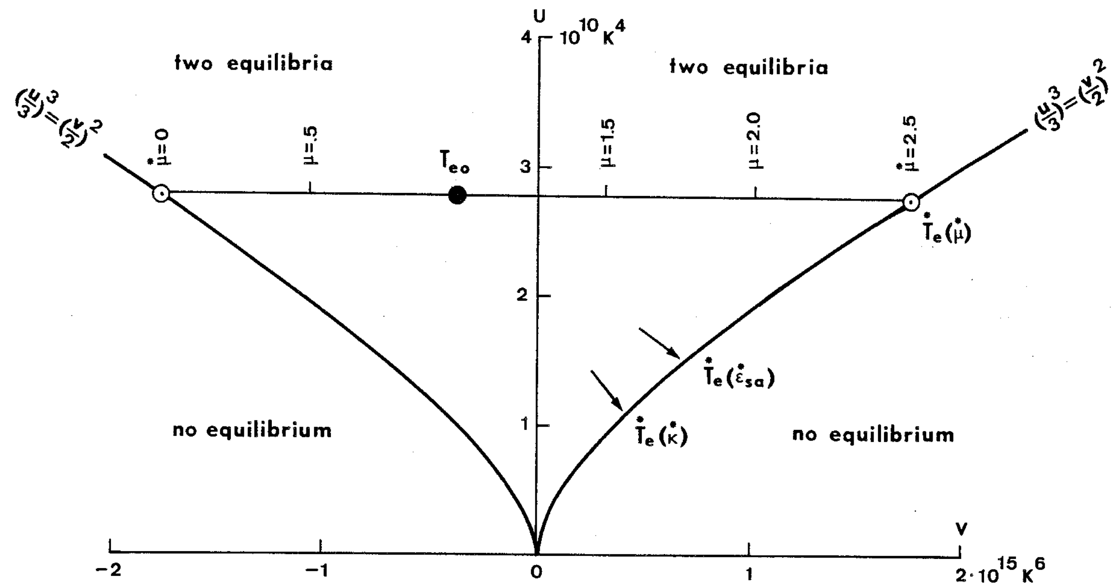

(iii) BIFURCATION DIAGRAM

Figure 4. Climate system with greenhouse effect: (a) equilibria (cross-section through state space); (b) phase portrait at reference conditions; (c) bifurcation diagram on parameter plane. (For detailed description see Fig. 3.)

abandoned when $v/2 > (u/3)^{\frac{3}{2}}$ or $\mu I_0(1-\alpha_p)/4\kappa\sigma > \frac{1}{2}(2\varepsilon_{sc}/3\kappa)^3$, so that 'desert heat' conditions are attained.

The geometrical interpretation of the attractor and repeller by the potential is obvious and has already been given in section 2; the same holds for the local maximum and minimum of the potential coinciding at the fold catastrophe. For a continuously decreasing greenhouse feedback (i.e. $\kappa \to 0$) the system (5.1) attains the structure of the trivial climate system (3.1). This can be visualized from Fig. 4 (equilibria) by $\overset{*}{T}_e \to \infty$ with $\overset{*}{\mu} \to \infty$ or $\kappa \to 0$. This behaviour is analogous to the continuously reduced ice-albedo feedback (section 4, $b \to 0$).

An example illustrates the structural behaviour of this climate system. From Eqs. (5.4), at $\lambda = 0$, and Eq. (5.2a) two conclusions can be directly drawn. At vanishing net incoming radiation ($R\!\downarrow\, = 0$; i.e. $\mu = 0$ or $\alpha_p = 1$) two equilibria appear: $T_e^- = 0$ and $T_e^+ = (\varepsilon_{sc}/\kappa)^{\frac{1}{2}}$, from which two equilibrium branches emerge with increasing solar radiation, For all other parameters fixed at 'present day' conditions these equilibria, $T_e(\mu)$, appear as a cross-section through the state space (Fig. 4(a)). They meet at the bifurcation point

$$\overset{*}{T}_e = +(2\varepsilon_{sc}/3\kappa)^{\frac{1}{2}}, \qquad (5.6)$$

where $\overset{*}{\mu} = 2{\cdot}5$ (Eq. (5.5)) and $\overset{*}{T}_e = 438\,\mathrm{K}$. Projected into an appropriate parameter space, the corresponding variations of solar radiation intensity are shown in Fig. 4(c), where they cross the fold lines at the bifurcation points. Bifurcation points for other external parameters can also be deduced from Eqs. (5.2) and (5.5). Some of them are indicated in Fig. 4(c).

Comparing the ice-albedo and greenhouse feedback mechanisms, a completely opposite structural behaviour appears, which is clearly exhibited by the geometry of the graphs (Figs. 3(a) and 4(a)). For fixed external parameters, resilience of the first kind shows that a stable equilibrium attracts the flow of the internal variable as it starts from initial values of a basin limited by an unstable equilibrium. For a positive greenhouse or negative ice-albedo feedback there exists only an upper or a lower bound (i.e. the repeller, unstable equilibrium) for the basin, beyond which the 'desert heat' or 'deep freeze' climate state is approached. This behaviour is forced by temperature variations solely within the system (e.g. due to internal fluctuations, if the repeller lies close enough to the attractor), without any external parameter change at all.

The structural behaviour (resilience of the second kind) shows that fold-lines separate the parameter plane into two areas: one with, and the other without, any stable equilibrium at all. At the bifurcation line itself the stable and unstable equilibria coalesce. Beyond the fold-catastrophe there is no real equilibrium. Thus, for the greenhouse or ice-albedo feedback there appears an upper or lower limit for the external parameter μ, beyond which the 'desert heat' or 'deep freeze' state is approached. These are catastrophes triggered by changes of the external parameters only.

In the following section the two feedback mechanisms are combined.

6. Ice-albedo and greenhouse feedbacks

Combination of the (quadratic) ice-albedo and greenhouse feedback mechanisms parameterized by Eqs. (2.4) and (2.6) leads to the following climate system:

$$dT/dt = (1/c)\{\kappa\sigma T^6 - \varepsilon_{sc}\sigma T^4 + \tfrac{1}{4}\mu I_0 b_2 T^2 + \tfrac{1}{4}\mu I_0(1-a_2)\} \quad . \qquad (6.1)$$

The equilibria satisfy the sixth-order polynomial $f(T_e) = 0$:

$$T_e^6 - T_e^4\,\varepsilon_{sc}/\kappa + T_e^2(\tfrac{1}{4}\mu I_0/\kappa\sigma)b_2 + (\tfrac{1}{4}\mu I_0/\kappa\sigma)(1-a_2) = 0, \quad . \qquad (6.2a)$$

which can be transformed to the following normalized cubic equation (see section 5):

$$y^3 - py + q = 0; \qquad y = -\varepsilon_{sc}/3\kappa + T_e^2, \quad . \quad . \qquad (6.2b)$$

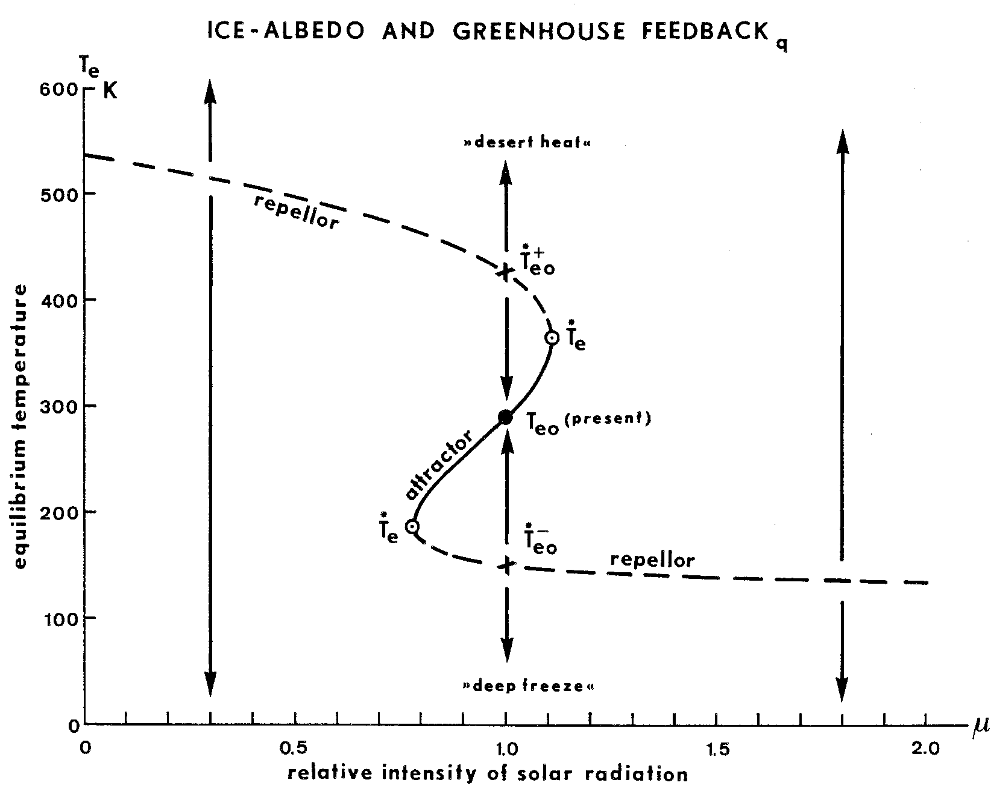

(a)

(i) EQUILIBRIA

(b)

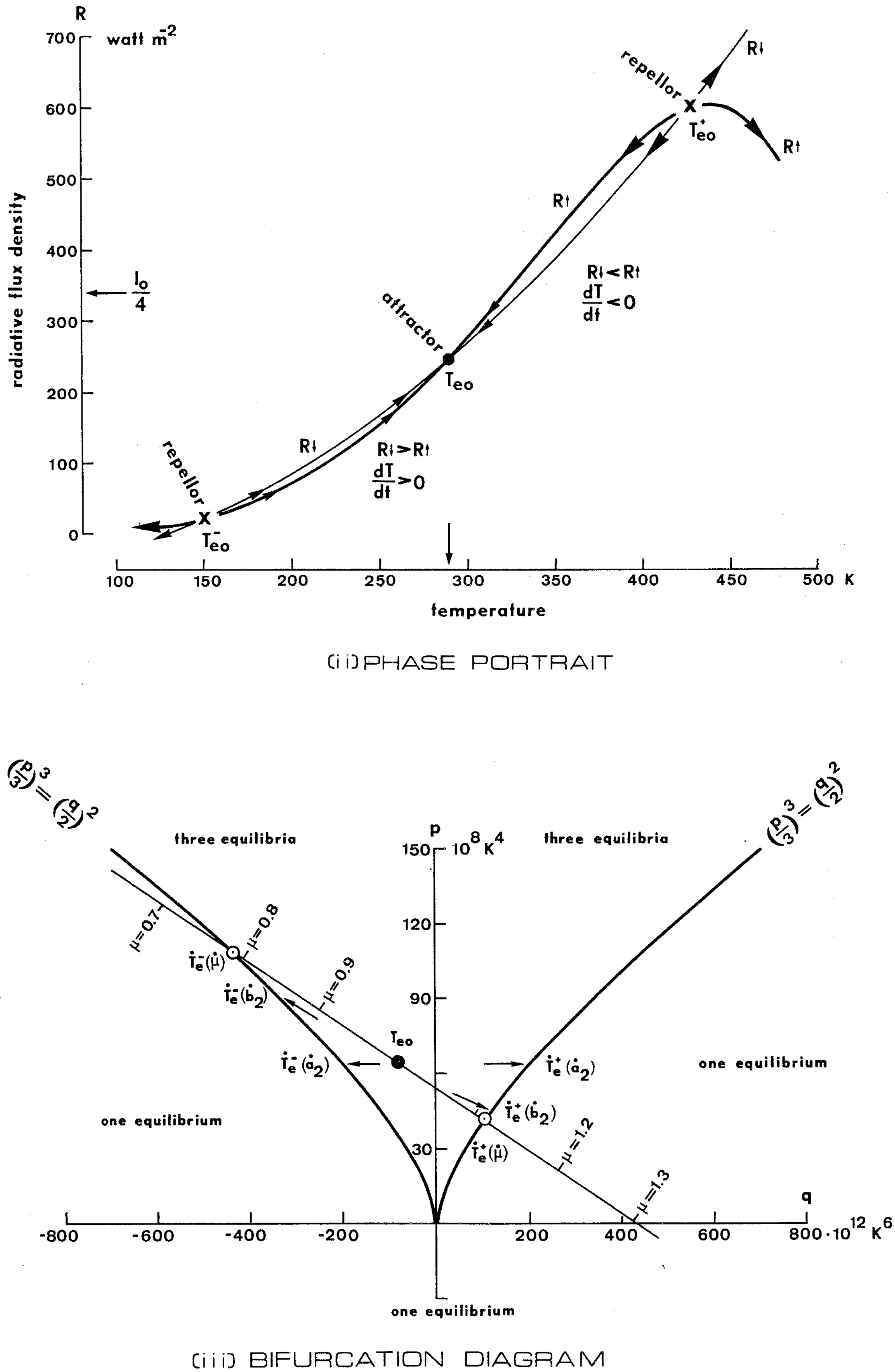

(c)

Figure 5. Climate system with combined ice-albedo and greenhouse feedbacks: (a) equilibria (cross-section through state space); (b) phase portrait at reference conditions; (c) bifurcation diagram on parameter plane. (For detailed description see Fig. 3 and text.)

where the definition of y is the same as in Eq. (5.2b), and

$$\begin{aligned} p &= 3(\varepsilon_{sc}/3\kappa)^2-(\tfrac{1}{4}\mu I_0/\kappa\sigma)b_2 \\ q &= -2(\varepsilon_{sc}/3\kappa)^3+(\varepsilon_{sc}/3\kappa)(\tfrac{1}{4}\mu I_0/\kappa\sigma)b_2+(\tfrac{1}{4}\mu I_0/\kappa\sigma)(1-a_2) \end{aligned} \quad . \qquad (6.2c)$$

The equilibria depend on the six external parameters $x = (a_2, b_2, \varepsilon_s, \varepsilon_c, \kappa, \mu)$, which can be reduced to two combinations (p,q), defining a parameter plane. The positive roots of Eqs. (6.2) yield the following equilibrium temperatures, producing a continuous surface in the state space $(T_e; p, q)$:

$$T_e = +\{\varepsilon_{sc}/3\kappa+2A(|p|/3)^{\frac{1}{2}}\}^{\frac{1}{2}} \quad . \qquad (6.3)$$

For $p > 0$ and $(q/2)^2 < (p/3)^3$ there exist three solutions with $A = \cos(\rho/3); -\cos\{(\pi+\rho)/3\}; -\cos\{(\pi-\rho)/3\}$ where $\rho = \mathrm{arc\,cos}\{-(q/2)(p/3)^{-\frac{3}{2}}\}$. For $p > 0$, $(q/2)^2 > (p/3)^3$ one (real) solution exists: $A = \cosh(\rho/3)$ where $\rho = \mathrm{Arcosh}\{-(q/2)(p/3)^{-\frac{3}{2}}\}$. For $p < 0$, there is another real solution: $A = \sinh(\rho/3)$ with $\rho = \mathrm{Arsinh}\{-(q/2)(p/3)^{-\frac{3}{2}}\}$.

All these solutions combined form the equilibrium set and are discussed in the following. In Fig. 5 the equilibria are presented for varying solar radiation intensity, μ, with all other external parameters fixed and defined by the reference situation (section 3). The internal stability of the complete set of the equilibria is given by

$$-\lambda = (df/dT)|_{T_e} = (\kappa\sigma/c)\{T_e^4-\tfrac{2}{3}T_e^2(\varepsilon_{sc}/\kappa)+(\tfrac{1}{4}\mu I_0/\kappa\sigma)(b_2/3)\}\,6T_e \begin{array}{l} < 0 \text{ stable} \\ > 0 \text{ unstable} \end{array} \qquad (6.4)$$

This criterion characterizes the upper and lower branches of the equilibria (Fig. 5) as unstable solutions (repellor). All solutions of the intermediate branch appear as stable equilibria (attractors). For all external parameters fixed at 'present day' conditions the phase portrait can be constructed (Fig. 5). It is seen that initial values attracted by the stable equilibrium, T_e, are bounded by the two repellors, T_e^+ and T_e^-. Beyond these, either the 'desert heat' or the 'deep freeze' state will be attained unless the greenhouse or ice-albedo feedbacks is cut off, e.g. by a constant atmospheric emittance ε_a or planetary albedo α_p.

For present day conditions the characteristic time scale for the system to approach the attractor T_{e0} yields $\tau_{c0} = \lambda_0^{-1} = 8{\cdot}1$ yr. As this time scale is represented by the difference $R\downarrow - R\uparrow$, it can be visualized in the phase portrait (see (iii) in section 2). Comparing the portraits of no feedback, and ice-albedo, greenhouse and combined feedback, we see that this difference is largest for no feedback (fast relaxation time scale) and smallest for the combined ice-albedo and greenhouse feedback (slow time scale) because the effects oppose each other, preventing a fast approach towards the attractor.

The equilibria can experience sudden changes in the state space $(T_e; p, q)$ due to small variations of the external parameters (p,q) only. As described by the condition of structural instability, fold catastrophes occur which can most simply be derived from the normalized equation (6.2b) and its first derivative by eliminating y:

$$(\tfrac{1}{2}q)^2 = (\tfrac{1}{3}p)^3 \quad . \qquad (6.5)$$

The related bifurcation temperatures, $\overset{*}{T}_e$, can be deduced from Eqs. (6.4), $\lambda = 0$, and (6.5).

The related parameter combination can be determined if (p,q) defined by Eq. (6.2b) are introduced into Eq. (6.5). The resilience, or prediction of the second kind, leads to the following results. If the singularities of the equilibria, as they occur in the $(T_e; p, q)$ state space, are projected on to the parameter plane (p, q), two lines of fold catastrophes, Eq. (6.5), appear (Fig. 5(c)). Sudden changes of the equilibria happen for parameters crossing these fold lines. They confine an area in the parameter plane (p, q) within which three

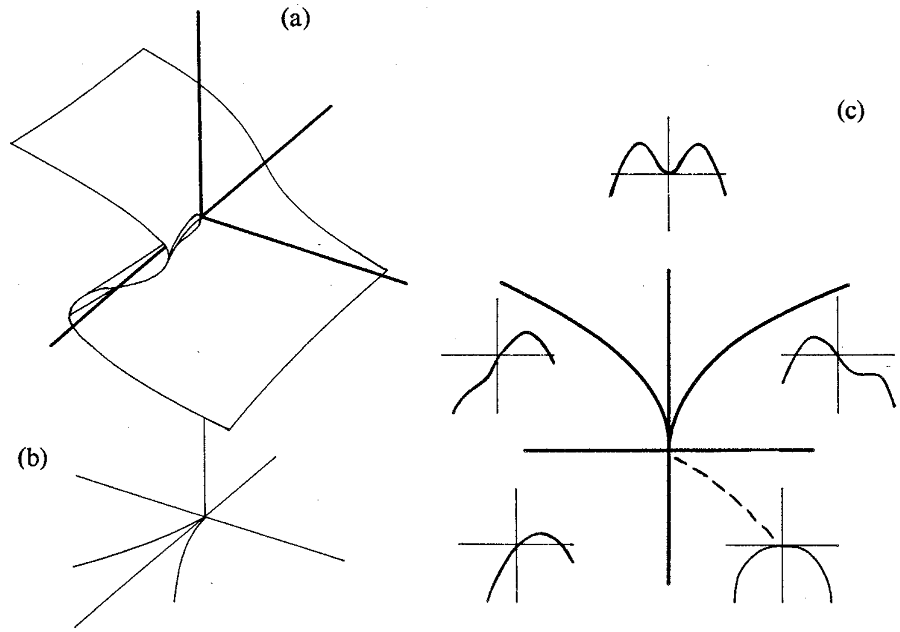

Figure 6. Sketch of (a) equilibria in the state space, (b) singularities of equilibria projected onto the parameter plane (bifurcation diagram), and (c) the potentials related to their positions in the bifurcation diagram.

equilibria $((q/2)^2 < (p/3)^3)$ in the state space $(T_e; p, q)$ exist simultaneously. One of these equilibria is an attractor which is framed by two repellors (Fig. 5(a)) the internal stability, Eqs. (6.4), of which has been discussed above. Everywhere else in the parameter plane, outside this area between $(q/2)^2 = (p/3)^3$, there is only one unique equilibrium set, which is internally unstable and therefore a repellor. Initial values above (below) this repellor lead to a temperature flow towards plus (minus) infinity, i.e. the 'desert heat' ('deep freeze') state.

Physically, the attractor can be interpreted as the interglacial climate separated from the 'desert heat' and the 'deep freeze' by two repellors (one above and one below the attractor). At fixed external parameters ('present day' condition) variations of the internal variable T (e.g. by weather fluctuations) can bring the system into a state of 'deep freeze' or 'desert heat' only if the variations are large enough. This describes the concept of resilience in the state space (prediction of the first kind). On the other hand, the interglacial attractor can also be abandoned by parameter variations, if these move beyond the catastrophic fold lines $(q/2)^2 = (p/3)^3$ into $(q/2)^2 < (p/3)^3$ or $p < 0$. Whether the climate system finally attains 'deep freeze' or 'desert heat' depends on the initial situation of the state variable (i.e. the initial condition) with respect to the repellors. This describes the concept of resilience of state space (prediction of the second kind). The geometrical interpretation by the potential becomes obvious from Fig. 6.

Two examples of structural analysis illustrate the behaviour of the system. If the relative intensity of solar radiation, μ, is assumed to change and all other parameters are kept fixed at 'present day' conditions, the equilibria appear as a cross-section through the $(T_e; p, q)$ space (Fig. 5(a)). The related variations of solar radiation intensity projected into the (p, q) parameter space (using Eq. (6.2b)) are shown in Fig. 5(c), where they cross the fold lines $(q/2)^2 = (p/3)^3$ at two bifurcation points for $\overset{*}{\mu}$:

$$(\tfrac{1}{4}\overset{*}{\mu} I_0/\kappa\sigma)(b_2/3) = \tfrac{1}{2}(\varepsilon_{sc}/3\kappa)^{\frac{1}{2}}[3 - \tfrac{1}{4}(A+3)^2 \pm \{(3 - \tfrac{1}{4}(A+3)^2)^2 + 4A\}^{\frac{1}{2}}]$$

where

$$A = 3\{(1-a_2)/b_2\}\{3\kappa/\varepsilon_{sc}\}; \qquad (6.6)$$

$$\overset{*}{T}{}_e^2 = (\varepsilon_{sc}/3\kappa)[1 \pm [(A+3)^2/8 - \tfrac{1}{2} \pm \{(3 - \tfrac{1}{4}(A+3)^2)^2 + 4A\}^{\frac{1}{2}}]^{\frac{1}{2}}];$$

i.e. for 'present day' conditions (section 3) the μ bifurcations lie at $\overset{*}{T}_e^+ = 365\,K$ for $\overset{*}{\mu}^+ = 1{\cdot}11$ and at $\overset{*}{T}_e^- = 187\,K$ for $\overset{*}{\mu}^- = 0{\cdot}78$. For $\mu \gtrless \overset{*}{\mu}^\pm$ there are no stable equilibria so that the system attains the 'deep freeze' or 'desert heat' state depending on the initial temperature lying above or below the repellors. Bifurcation points for other external parameters can also be deduced from Eqs. (6.2c) and (6.5). Some of them are indicated in Fig. 5(c), where the remaining external parameters are fixed at 'present day' conditions.

The other point of interest in the parameter plane (p, q) is the cusp (section 2) where the two bifurcation lines or fold catastrophes meet. From the normalized condition (6.2b) they meet at the origin $p = q = 0$. Considering all the external parameters x one obtains for the cusp (2.11):

$$1 = (-\tfrac{1}{4}\mu I_0/\kappa\sigma)(1-a_2)(3\kappa/\varepsilon_{sc})^3 \quad \text{and} \quad \varepsilon_{sc}/3\kappa = 3(1-a_2)/(-b_2). \tag{6.7}$$

The related equilibrium temperature is given by

$$\hat{T}_e = (\varepsilon_{sc}/3\kappa)^{\frac{1}{2}} \quad . \quad . \quad . \quad . \tag{6.8}$$

For example, at 'present day' ε_{sc0} and κ_0, the cusp temperature yields $\hat{T}_e = 309\,K$.

From the analysis of this section it can be seen how the ice-albedo and greenhouse feedbacks (sections 4, 5), after combination, keep their own structural behaviour. If the greenhouse effect becomes too strong the upper bifurcation point, $\overset{*}{T}_e^+$, moves towards higher temperatures; if the ice-albedo feedback becomes too strong, the lower bifurcation point, $\overset{*}{T}_e^-$, moves towards lower temperatures. The bifurcation points may coincide (cusp), or even vanish, if the feedbacks balance each other. Then the climate system consists of unstable solutions only. This is just the opposite behaviour to the case of no feedback (shown in section 3). All other cases are intermediate, as shown by the example presented in Fig. 5.

7. Sensitivity and stochastic feedback

As discussed in the earlier paper (Fraedrich 1978) the sensitivity of the climate system can be defined by the internal climate variable responding linearly to relative changes of one of the external parameters, x (e.g. at the conditions of the stable equilibrium):

$$\beta_x = (\partial T_e/\partial \ln x)|_{x_0} \quad . \quad . \quad . \tag{7.1}$$

The sensitivity parameter β is determined for two external parameters currently of interest: the relative intensity of solar radiation, μ, and the CO_2 content. The latter is given by

$$\beta_{CO_2} = (\partial T_e/\partial \ln\varepsilon_c)(\partial\varepsilon_c/\partial \ln CO_2) = 0{\cdot}0235\,\partial T_e/\partial \ln\varepsilon_c \quad . \tag{7.2}$$

At 'present day' conditions these sensitivities are calculated for the climate systems discussed in the sections 3 to 6: the trivial, the ice-albedo feedback, the greenhouse effect and the combined feedback model. The results are collected in Table 1, where the temperature change of $0{\cdot}01\beta$ is due to a one per cent change of the external parameter about the reference state. In addition, this table summarizes some of the information characterizing the climate systems and shows how they differ: the linear time scale $\tau_c = \lambda^{-1}$, the bifurcation temperatures, $\overset{*}{T}_e(\overset{*}{\mu})$, due to solar radiation changes, and the repellor temperatures at 'present day' condition. Finally, the temperature response of the linearized versions of the climate systems (section 2) on stochastic forcing (Fraedrich 1978, sections 5 and 6 and Figs. 4 and 5) can be determined from related Langevin-type climate equations. The white noise input, D, into the Langevin climate equations is due to short-period weather fluctuations. These are assumed to work on an energy flux level of one percent efficiency ($\eta = 0{\cdot}01$) which is con-

TABLE 1. SUMMARY OF INFORMATION FROM THE ANALYSIS OF THE ZERO-DIMENSIONAL CLIMATE SYSTEMS

Feedback	Sensitivity (K) β_μ	Sensitivity (K) β_{CO_2}	Bifurcation $\overset{*}{T}_e(\overset{*}{\mu})$ (K)	Bifurcation $\overset{*}{\mu}$	Repellor about present day (K) $T_{e0} = 288{\cdot}6$ K	Time scale (yr) $\tau_c = \lambda^{-1}$	Stochastic temperature response: $(2D/\lambda)^{\frac{1}{2}}$ (K)	Remarks
No feedback	72	1·7	0	0		1·4	0·28	—
Ice-albedo	191	4·5	180	0·63	142	2·4	0·45	'deep freeze'
Greenhouse	90	3·0	438	2·5	518	1·8	0·31	'desert heat'
Ice-albedo plus greenhouse	413	13·7	365	1·11	456	8·1	0·66	'deep freeze'
			187	0·78	151			'desert heat'

verted from the net incoming radiation $R\downarrow$ after a characteristic time scale of 25 days $\ll \tau_c$ (blocking activity). Thus, $D = 2{\cdot}7 \times 10^{-2}\mathrm{K}^2\mathrm{yr}^{-1}$. It can be shown that the Langevin-type climate systems attain the maximum standard deviation $(2D/\lambda)^{\frac{1}{2}}$ of their temperatures after a sufficiently long averaging time, $\gg \tau_c$. These values are presented in Table 1. As long as the repellor temperatures are far from the 'present day' equilibrium 288·6 K, weather fluctuations (as they are parameterized here) can hardly 'push' the climate system out of the (interglacial) basin. But the external parameters can be changed slightly such that the repellors narrow the basin. Then, unless the stochastic forcing is diminished simultaneously, an unstable parameter and state variable combination can more easily be approached.

Overall comparison shows that the faster reacting systems (e.g. no feedback) have smaller responses on stochastic forcing and also a smaller sensitivity. This is due to the fact that the linear plane tangent to the nonlinear equilibrium temperature surface of the no feedback system is hardly sloped in the state space compared to the combined ice-albedo plus greenhouse feedback model. These slopes increase the closer the bifurcation point, or temperatures (e.g. for μ), lie to the 'present day' equilibrium condition x_0 or temperature $T_{e0} = 288{\cdot}6\,\mathrm{K}$.

8. Conclusion

An almost trivial climate system has been investigated in this paper and a previous one (Fraedrich 1978) applying a gradient system approach to climate modelling. There are two aspects, which may be called chance and necessity (stochastic and deterministic), cooperating to achieve the climate variations of this system. Correspondingly, two related concepts of resilience (or predictions of the first and second kinds) are introduced to separate these two viewpoints. Analysis according to one of the concepts (resilience of the second kind) classifies the qualitative structure of the system which eventually becomes unstable at critical external parameter combinations; such a structural analysis of gradient systems (called elementary catastrophe theory) is also known for its possible applicability to the simulation of complex natural phenomena. But there is presently discussion about applied catastrophe theory (e.g., Zeeman 1976; Zahler and Sussmann 1977), which mainly refers to the (often very intuitive) construction of models describing biological, social, etc., phenomena such that necessarily a gradient system is obtained exhibiting one of the seven elementary catastrophes. However, the development of systems (like this climate system) from a basic physical law and experimentally verified parameterizations is a different type of model construction. Furthermore, another aspect is added to the analysis by the internal dynamics of the system and its stability at fixed external parameters. This leads to the resilience of the first kind and appears directly from analysing simple gradient systems; i.e. at fixed external parameters the system develops deterministically but the flow depends on the initial conditions. These, however, can well be posed by chance (e.g. by internal fluctuations). The two concepts combined lead to the complete view of this climate system, its structure and stabilities. For systems with more complex dynamics than the gradient system, however, there may occur cycles or strange attractors.

Acknowledgments

Thanks are due to Ms M. Lungwitz, U. Eckertz-Popp, and Mr H. Haug for typing, photographing and drafting. The discussions with Dr H. R. Grümm, and the calculations by Mr A. Behlau are appreciated.

References

Bröcker, T. 1975 Differential germs and catastrophes, London Mathematical Society, *Lecture Note Series* 17.

Bryson, R. A. and Dittberner, G. J. 1976 A non-equilibrium model of hemispheric mean surface temperature, *J. Atmos. Sci.*, **33**, 2094–2106.

Budyko, M. I. 1969 The effect of solar radiation variations on the climate of the earth, *Tellus*, **21**, 611–619.

Deacon, E. L. 1970 The derivation of Swinbank's long-wave radiation formula, *Quart. J. R. Met. Soc.*, **96**, 313–319.

Fraedrich, K. 1978 Structural and stochastic analysis of a zero-dimensional climate system, *Ibid.*, **104**, 461–474.

Grümm, H. R. 1976 Definitions of resilience, IIASA RR–76–5, International Institute of Applied Systems Analysis, Laxenburg, Austria.

Holling, C. S. 1973 Resilience and stability of ecological systems, *Annual Review of Ecology and Systematics*, **4**, 1–23.

Lian, M. S. and Cess, R. D. 1977 Energy balance climate models: a reappraisal of ice-albedo feedback, *J. Atmos. Sci.*, **34**, 1058–1062.

Lorenz, E. N. 1975 Climate predictability, World Meteorological Organization *GARP Publ. Ser.*, **16**, 132–136.

Raschke, E., Vonder Haar, T. H., Bandeen, W. R. and Pasternak, M. 1973 The annual radiation balance of the earth–atmosphere system during 1969–70 from Nimbus 3 measurements, *J. Atmos. Sci.*, **30**, 341–364.

Sellers, W. D. 1969 A global climatic model based on the energy balance of the earth–atmosphere system, *J. Appl. Met.*, **8**, 392–400.

Swinbank, W. C. 1963 Long-wave radiation from clear skies, *Quart. J. R. Met. Soc.*, **89**, 339–348.

Thom, R. 1975 Structural stability and morphogenesis, Benjamin Inc.; Reading, Mass.

von Woerkom, A. J. J. 1953 The astronomical theory of climate changes. In *Climatic change*. Harvard University Press, Cambridge, 147–157.

Zahler, R. S. and Sussmann, H. J. 1977 Claims and accomplishments of applied catastrophe theory, *Nature*, **269**, 759–763.

Zeeman, E. C. 1976 Catastrophe theory, *Sci. Amer.*, **234**, 65–83.

Appendix

List of symbols

T; t	temperature (internal variable); time
$R\downarrow$, $R\uparrow$, $L\downarrow$, $L\uparrow$	radiation fluxes
μI_0; α_p	solar radiation, I_0 being the solar constant; planetary albedo
σ	Stefan–Boltzmann constant
a, b	albedo–temperature feedback coefficients
ε_a, ε_c, κ	greenhouse effect coefficients
ε_s, ε_{sc}, ε_{sa}	surface emissivity; $\varepsilon_{sa} = \varepsilon_s - \varepsilon_a$, $\varepsilon_{sc} = \varepsilon_s - \varepsilon_c$
c; c_m, ρ_m, h, α	thermal inertia; specific heat, density, depth, area cover of an ocean layer
x	external parameters: $(a, b, \varepsilon_s, \varepsilon_a, \varepsilon_c, \kappa, c, \mu)$
m, n; u, v; p, q; ρ, A	combinations of external parameters
f, V	climate equations: gradient system, potential
λ	eigenvalue
$\tau_c = \lambda^{-1}$	climatic time scale
β_x	sensitivity parameter

Suffixes and indices

e, 0	equilibrium, reference ('present day') climate
*, $\hat{}$	bifurcation, cusp